Tsunami Vulnerability Function Development Based on the 2011 Tohoku Earthquake in Japan

Manabu Masuda, Chesley Williams, Ali Shahkarami, Farhat Rafique Jason Bryngelson

Risk Management Solutions, Inc. , USA

Tamiyo Kondo

Kobe University, Japan

SUMMARY:
Catastrophe risk models have been widely accepted and used by the insurance and reinsurance industries over past decades as a means to quantify and manage risk. However, tsunami risk has not been fully incorporated into most commercially-available catastrophe models because historical records are limited and the modelling is highly complex. The tragic 2011 Tohoku Earthquake destroyed many beautiful cities, towns, and villages, killed more than 19,000 people, devastated regional economies, and impacted the global economy, but it also provided new data that can be used to better understand and quantify the tsunami risk and to prepare for tsunamis in the future. This paper presents a set of tsunami vulnerability functions that are based primarily on observations from the Tohoku earthquake. Vulnerability classifications include key building attributes such as construction type, occupancy class, and building height.

Keywords: Tsunami vulnerability; 2010 Tohoku earthquake; Catastrophe risk model

1. INTRODUCTION

Tsunami vulnerability has been studied in Japan by many researchers over the years. The most well-referenced and widely used vulnerability measurement is the one proposed by Shuto (1993), which estimates expected damage versus inundation depth for different building types. The relationships are primarily derived from post-event damage surveys following tsunami events. Many scenario loss simulations and emergency response manuals published by federal and local governments have used these relationships to estimate potential tsunami losses. After the 2004 Indian Ocean Tsunami, several fragility studies were published by incorporating numerical tsunami simulation models, damage assessments using remote sensing technology (e.g. Koshimura et al., 2009) and inundation flow velocity (e.g. Iizuka and Matsutomi, 2000 and Matsutomi et al., 2010). However, because of the lack of high-resolution loss information, studies have been limited to the development of fragility curves (exceedance probability for given damage state and intensity) or vulnerability functions for specific construction classifications, which might not be applicable to buildings in other countries. Also, the current available tsunami damage functions are not fully calibrated or reviewed for regional portfolio loss estimation. In this paper, the authors discuss the process of developing a catastrophe model, which includes hazard, vulnerability, exposure, building inventory and loss estimation. The proposed tsunami vulnerability functions are used to examine the potential impacts of several key tsunami scenarios in Japan, including the 2011 Tohoku earthquake on the Japan Trench, as well as Tokai and Tonankai scenario events on the Nankai Trough. The results and proposed vulnerability functions can be used by the insurance industry and by government agencies to manage and mitigate tsunami risk in the future. The paper begins with a summary of the damage statistics from the 2011 Tohoku earthquake and how this high-resolution information is used to develop vulnerability functions for tsunami hazard.

2. DAMAGE STATISTICS

2.1. Published Damage Statistics

Vulnerability development for tsunami hazard requires high quality data sets for three key components of a catastrophe model: hazard (inundation depths), exposure (type and location of property) and damage (mean damage ratio or another quantitative measure). A number of reconnaissance reports and damage statistics have been published since the 2011 Tohoku earthquake by academia, Japanese structural (AIJ) and civil engineering (JSCE) associations, and government agencies. Among these, the damage survey report published by the Ministry of Land, Infrastructure, Transport and Tourism (MLIT) includes the most comprehensive information on buildings damaged by tsunami only. For validation purposes, the numbers of damaged and inundated residential buildings in the report are compared with those from damage statistics compiled by the Fire and Disaster Management Agency (FDMA) in Table 2.1, as the FDMA data are the most-referenced data. Because the FDMA data include buildings damaged by both shake and tsunami, it should be noted that the comparison is not a direct one and these statistics are not considered to be final. However:

- Overall numbers are comparable, though many inundated (above first floor [1F] level) buildings are classified as "partial damage" in the FDMA statistics.
- Differences in definitions of building count, occupancy and damage state might have resulted in some inconsistencies between the two datasets.
- Shake damage is overshadowed by tsunami damage, but it is still significant.

Table 2.1. Number of damaged residential buildings in MLIT and FDMA reports

Organization	City Bureau, MLIT			FDMA[1]			FDMA [1]		
Coverage	within Tsunami footprint			cities impacted by the tsunami			all cities/wards		
Peril	Tsunami Only			Shake and Tsunami			Shake and Tsunami		
Prefecture	Structural Damage[2]	Inunda -ted	Total	Structural Damage[2]	Inunda -ted	Total	Structural Damage[2]	Inunda -ted	Total
Aomori	877	1,730	2,607	1,280	0	1,280	1,285	0	1,285
Iwate	27,594	4,246	31,840	25,244	2,083	27,327	32,052	2,083	34,135
Miyagi	86,880	34,156	121,036	151,659	19,193[3]	170,852	433,748	19,199	438,442
Fukushima[4]	7,142	5,233	12,375	94,864	1,331	96,195	223,872	1,393	225,265
Ibaraki	425	3,485	3,910	80,908	1,467	82,375	191,550	2,426	193,976
Chiba	1,230	1,707	2,937	9,505	61	9,566	54,119	875	54,994
Total	124,148	50,557	174,705	363,460	24,135	387,595	936,626	25,976	948,097

Notes

1) FDMA: Report #143 as of January 11th.
2) Structural Damage: Total collapse, half collapse and partial damage.
3) Official numbers from heavily-impacted cities have not been reported yet.
4) More than a few cities/wards have data quality issues near the Fukushima Nuclear Power Plants.

2.2. MLIT Damage Survey Report Summary

This dataset was included in the series of 2011 Tohoku earthquake damage survey reports compiled by the City Bureau of MLIT, which are prepared for recovery and rehabilitation planning in heavily impacted regions and for future loss mitigation. Detailed damage statistics by inundation heights are published in their Phase I and II reports. The database information regarding extent of damage, building attributes and usage was collected by field surveys conducted by local government officials. Also, the information was cross-referenced with the information in damage certificates. Kobe University and RMS collaborated for the future disaster mitigation planning and MILT generously provided their data set in digital format. The database covers 6 prefectures and 62 wards (shi, ku, cho and son) that consist of approximately 230,000 buildings. Figures 2.1 and 2.2 show the number of buildings and floor area by occupancy type, respectively, for each prefecture in the inundated zone. The inundation area covers approximately 540km^2 and water depth exceeded 2m in 40% of the total inundated area. More than 60% of measurements are collected in the Miyagi Prefecture and the predominant construction and occupancy classifications are wood and residential, as summarized in Table 2.2.

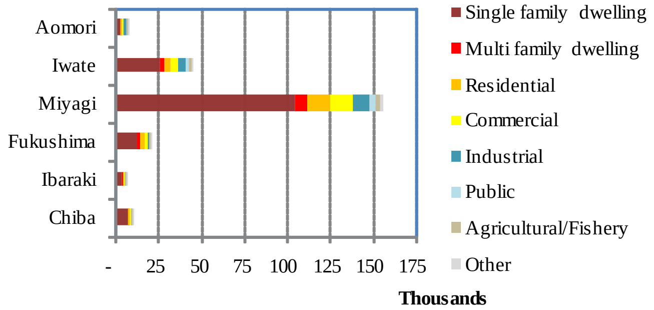

Figure 2.1. Number of buildings within inundated zones by occupancy

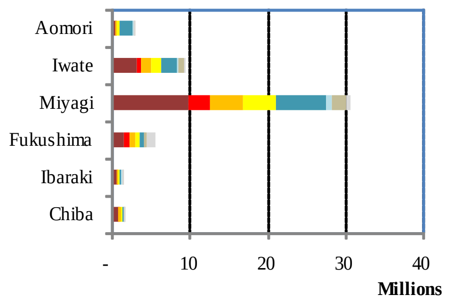

Figure 2.2. Total floor areas within inundated zones by occupancy

2.3. Building Classifications

Building classifications used in the dataset are summarized Table 2.2, which includes the total number of buildings within the inundated area. Based on these classifications, we developed 76 primary tsunami damage functions having different combinations of heights, construction and occupancy classifications. Damage state definitions in Japan specifically for water-related damage, including inland flood and surge risks, are unique (i.e., different from those in the U.S. and Europe), as summarized in Table 2.3. Unlike damage states commonly used for earthquake or hurricane risk assessment, the hazard component (inundation depth, such as 'above 1F' or first floor level) is embedded in the damage state definitions, assuming high correlation between hazard and loss.

Table 2.2. Primary Building Characteristics in the Damage Database

Construction Type	# of Bldgs	Height	# of Bldgs	Occupancy[1]	# of Bldgs
Reinforced Concrete (RC)/SRC	5,319	1F	52,826	Residential (SFD/MFD)	182,285
Steel (excl. Light Metal)	11,474	2F	68,675	Commercial	19,436
Wood	172,783	3F	2,932	Industrial	18,029
Other (LM, Masonry)	16,176	4F	790	Public	6,306
Unknown	31,620	5F	403	Agricultural/Fishery	4,587
		6F+	254	Unknown	6,729
		UNK	111,492		

Notes: 1) 15 sub-occupancies are available in the original report.

Table 2.3. Damage State Classifications

Code	Damage State	Description (MLIT)	# of Bldg	DS_DR
D1	Total Collapse (Wiped)	Buildings completely washed away	82,986	100%
D2	Total Collapse	Only building structures left. It is not financially reasonable to rebuild.	30,388	100%
D3	Total Collapse (Inundated 1st floor ceiling level)	Water reached above 1st floor ceiling level. It required major effort to reconstruct buildings in this category.	9,096	90%-100%
D4	Major Half Collapse	Water level exceeded 1m above 1st floor level but lower than 1st floor ceiling level.	35,175	60%-90%
D5	Half Collapse (Inundated above 1st floor level)	Water level was between 1m above 1st floor level and 1F level. (Minor repair costs expected)	39,441	40%-60%
D6	Partial Damage (Inundated below 1st floor)	Water level did not reach 1st floor level. (Only debris removal is required to be operational)	21,532	10%-40%
D7	No Damage	No damage	12,298	0%-10%
D0	Unknown	Unknown	6,456	Unknown

2.4. Damage State Mapping in the MLIT Report

Although recent advancements in remote sensing technology allow for some approximation of building damage using satellite imagery, the challenge remains to develop accurate damage state mapping, especially for minor to moderate damage as it is not easily identified by satellite images and is usually repaired much faster in less-impacted regions. As shown in Figure 2.3, more than 80% of damage is classified using visual observations from field surveys or from damage certificates. A snapshot of the high-resolution damage data from Ishinomaki-shi is shown in Figure 2.4. To capture location-level water depths, we generated a 100m-grid inundation footprint using more than 5,000 observation data points published by the Disaster Prevention Research Institute (DPRI) at Kyoto University as described in Section 5.

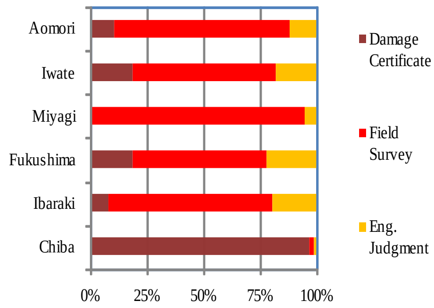

Figure 2.3. Data sources for damage state mapping

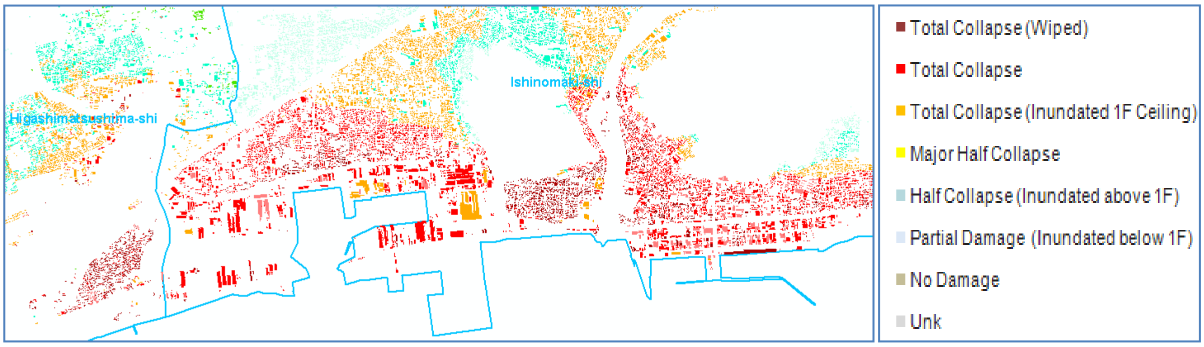

Figure 2.4. Damage state mapping, Ishinomaki-shi

3. VULNERBILITY DEVELOPMENT

3.1. Methodology

It is a common practice in earthquake and hurricane catastrophe modelling to use a combination of empirical and analytical approaches to develop vulnerability functions for different classes of buildings. With the acquisition of such a comprehensive damage data set described in Section 2, we primarily used an empirical approach to develop vulnerability functions, which requires fewer assumptions as compared to an analytical approach when the number of samples is large. An engineering approach using induced hydrodynamic forces and the expected seismic lateral load will be briefly discussed in Section 3.3. The application of an analytical approach must be developed in conjunction with numerical tsunami simulation model in order to incorporate a velocity component.

The vulnerability development consists of five steps:

1. The RMS engineering team joined with Japanese partners from Kajima Corporation to survey heavily-impacted regions inland and along coastal areas after the Tohoku earthquake. The teams visually investigated the relationship between tsunami extent and damage to various types of buildings and their contents.
2. Pre-earthquake exposure for each individual building within the inundation zones in six prefectures was created by processing GIS files provided by MLIT and incorporating reconstruction cost information (as described in Section 4). During this process, all building attributes were carefully reviewed and the data quality was enhanced by removing deficient data points and by including additional information based on common engineering/construction practices in Japan.

3. Inundation depths were assigned to each building by superimposing a high resolution (100m grid) tsunami footprint that was developed primarily based on observations (Section 5). An observed loss was estimated for each building by multiplying building value and mean damage ratios assigned to each damage state (DS_MDRs) as summarized in Table 2.3.
4. Observed losses and total building values were grouped into a set of water depth bins that are 0.5m or greater. Figure 3.1 shows the exposure-weighted damage state contributions for wood buildings in the inundation zone. Mean damage ratios for each water depth interval were computed from total estimated losses and total values in each bin to derive a vulnerability function for the selected classification. The mean damage ratio for each bin is defined in equation 3.1. Lognormal or beta distribution functions are commonly fit to represent damage functions with regression analyses, but a moving average was used to smooth the curves in order to retain damageability from the damage statistics especially at lower water depths. Figures 3.2 and 3.3 illustrate a vulnerability function and the distributions of number of samples for the single-story wood structure.
5. A suite of vulnerability functions was tested by comparing modelled numbers of damaged buildings to economic and insured losses (Section 5.4).

$$MDR_{depth} = \frac{\sum_1^n BldgValue_i \times DS\_MDR(Bldg_i)}{\sum_1^n BldgValue_i} \quad (3.1)$$

Where DS_MDRs are mean repair costs for given damage states.

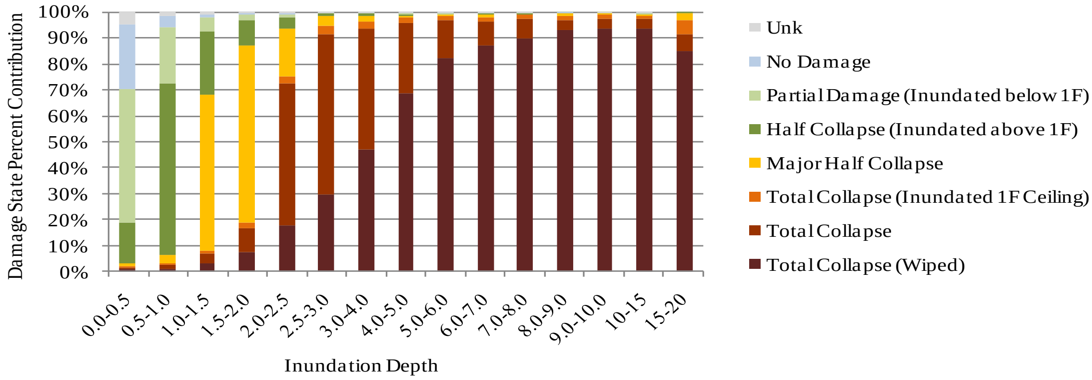

Figure 3.1. Exposure-weighted damage state contribution by inundation depth bin for wood structure

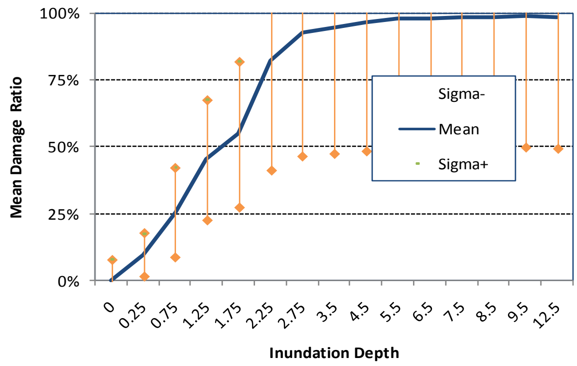

Figure 3.2. Mean damage ratio for single-story wood structure

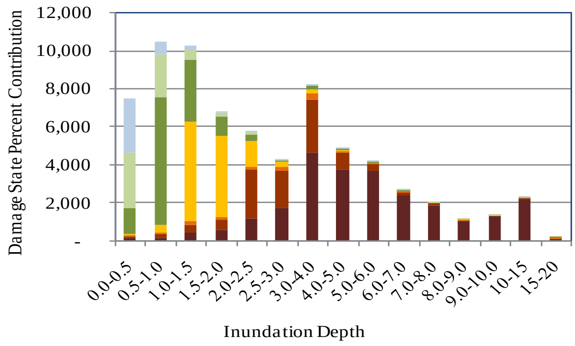

Figure 3.3. Number of samples for single-story wood structure

3.2. Observations

The empirically-based fragility functions indicate that the exceedance probability of collapse (D1-D3) significantly increases at water levels above 2m, especially for wood and light metal construction. The steps described in Section 3.1 were used to develop all 76 primary tsunami damage functions and

Figures 3.4 and 3.5 include examples of relative vulnerability by construction and height. Similar to surge/flood functions, tsunami functions are very sensitive to construction and height. Wood construction is the most vulnerable construction class, which does not withstand water depth above 2m regardless of its height. It appears that overall high water velocity in this event resulted in insignificant differences between the performance of 1F and 2F buildings. The data also show that occupancy was insignificant in estimating building damage. However, contents functions vary significantly by occupancy, which are incorporated in the model based on surge/flood functions proposed by the U.S. Army Corps of Engineers (USACE). The developed damage functions are compared with those proposed by Shuto (1993), Iizuka and Matsutomi (2000), Hattori (1964) and USACE in Figure 3.6. They match well, especially for wood buildings.

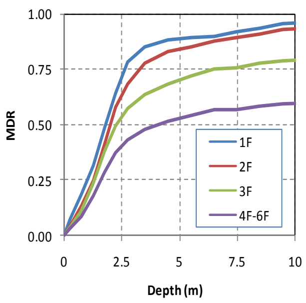

Figure 3.4. Relative vulnerability by height, single story all LOBs

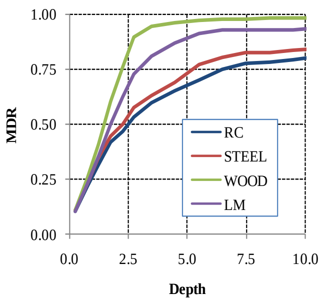

Figure 3.5. Relative vulnerability by construction, residential (SFD & MFD) buildings

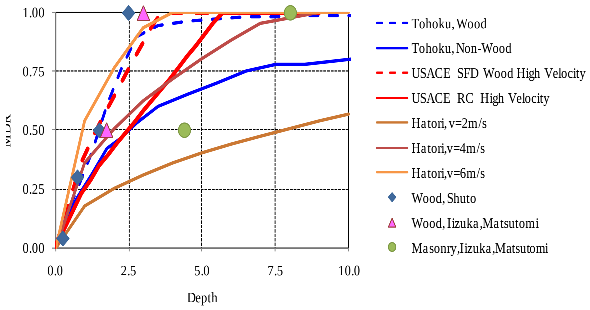

Figure 3.6. Tsunami damage function comparison

3.3. Reinforced concrete building vulnerability development using the IS index (seismic index defined in Japanese building code)

Although many mid-rise and high-rise reinforced concrete buildings were severely damaged during the earthquake, their damage mechanisms were not easily understood because they were driven by location-specific conditions such as building dimensions, types of exterior walls, wall openings, incoming/outgoing flow velocities, buoyant forces, and impact from debris. In this paper, a simplified approach using the IS index is proposed based on experience from seismic risk loss modelling. In this approach, the estimated building seismic lateral load is compared to the maximum hydrodynamic force of different water depths to estimate mean damage ratios. In the Japanese seismic evaluation guideline, the IS index is commonly used to evaluate the structural performance as a product of building strength and ductility index. The first step in this approach is to generate fragility functions for a given IS. The IS-Damage relationship introduced in Okada et al. (1988) is modified using damage statistics from the 1995 Kobe Earthquake. The detailed development procedure is discussed in Beck J. et al. (2002). Table 3.1 summarizes parameters for base IS damage distributions. The probability that the damage of a building with IS=x would exceed the damage state F when an earthquake with PGA = *a* occurs is:

Table 3.1. Base lognormal IS and fragility functions

	General IS Distribution	Damage State		
		Minor	Moderate	Major
y=ln(x)	-0.281	-0.64	-0.73	-0.87
σy	0.390	0.390	0.366	0.354

$$P(F \mid Is = x, A = a) = P(F \mid x, a) = \frac{P(x \mid F, a) \cdot P(F \mid a)}{P_{IS}(x)} \qquad (3.2)$$

Where $P_{Is}(x)$: IS distribution function of the building stock
$P(x|F,a)$: IS distribution function with the damage exceeding the damage state F for PGA=*a*.
$P(F|a)$: The probability that the building damage exceeds the damage state F for PGA=*a*.

$$\bar{y}(a) = \bar{y}(PGA_{BM}) + \frac{\bar{y}(a_u) - \bar{y}(PGA_{BM})}{1 - P(F \mid PGA_{BM})}\{P(F \mid a) - P(F \mid PGA_{BM})\}$$
$$\sigma_y(a) = \sigma_y(PGA_{BM}) + \frac{\sigma_y(a_u) - \sigma_y(PGA_{BM})}{1 - P(F \mid PGA_{BM})}\{P(F \mid a) - P(F \mid PGA_{BM})\} \tag{3.3}$$

Where $P(F \mid PGA_{BM}) = 0.210$, $\bar{y}(PGA_{BM}) = -0.73$ (for moderate), $\sigma_y(PGA_{BM}) = 0.366$, $\sigma_y(\alpha_u) = 0.499$
$PGA_{BM} = 0.6g$ (Benchmark PGA used for the base fragility curves based on the Kobe earthquake)

By linearly interpolating the mean and standard deviation using equation 3.3, IS fragility distributions can be obtained for given ground motion (PGA) as shown Figures 3.7 and 3.8. Damage functions (PGA-MDR) can then be computed by applying damage ratios associated with each damage state (minor=10%; moderate=30%; major=75%). Finally, mean damage ratios (MDRs) for given a IS, water velocity, and water depth are developed by relating estimated induced seismic lateral load and hydrodynamic force using equation 3.4. Figure 3.9 shows estimated MDRs for a 3-story reinforced concrete building (30m by 30m, 12kN/m^2 and Ds=0.5) for different IS values with 6m high water depth. Although the methodology requires further enhancements, it provides insights for loss estimates, taking into account the relationship between tsunami loads and building performance.

$$\mathrm{PGA} \times 2.5 \times \mathrm{Ds} \div \mathrm{g} \times \mathrm{Wt} = \frac{1}{2} \mathrm{C_D} \rho \max\left(\mathrm{v}^2 \mathrm{d}\right) \times \mathrm{B} \tag{3.4}$$

where D_S = ductility index, Wt = building weight, C_D = drag coefficient, v = water velocity, d = inundation depth and B = building length perpendicular to the water flow direction.

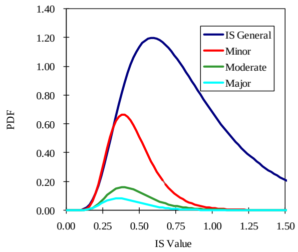

Figure 3.7. IS fragility distribution for PGA=0.4g

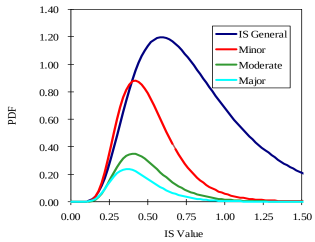

Figure 3.8. IS fragility distributions for PGA=0.8g

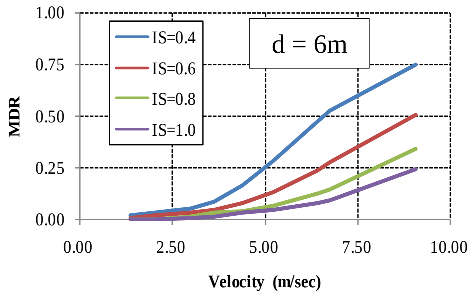

Figure 3.9. Tsunami damage functions for RC 3F (30m x 30m, 12kN/m^2, Ds=0.5)

4. EXPOSURE AND INVENTORY DEVELOPEMTNT

4.1. Exposure Assumptions

Exposure and building inventory development is a key component of catastrophe modelling. Depending on the availability of information and geographic resolution to study, practical assumptions must be made to estimate total values in regions. In the 2011 Tohoku earthquake, MLIT building footprints with associated construction type, occupancy, height and building footprint area were available. As described in Section 2, most primary building characteristics are given with building footprint areas. Accordingly, the only assumptions required to estimate property values are unit construction costs by building attributes which can be derived using publically-available

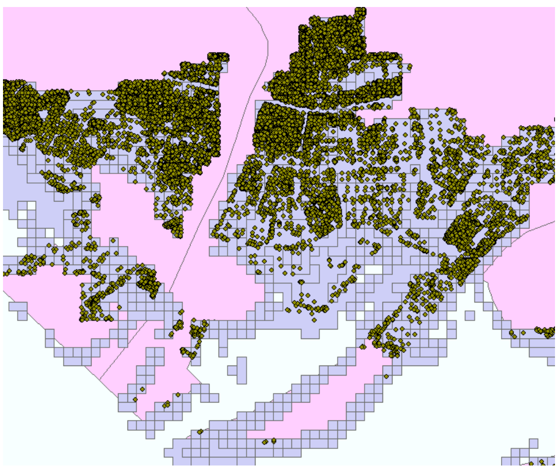

Figure 4.1. Location level high resolution exposure near Osaka Bay

information. The “construction year books” were used, which include newly-constructed floor areas and total project costs by occupancy (9 classes), construction (6 classes) and height (9 classes) in each city/ward, to estimate unit costs. Floor unit costs summarized in Table 4.1 are CPI (consumer price index) trended 7 year averages from 2004 to 2010 values. Recommended unit cost assumptions by one Japanese insurer are included for reference. Note that the types M (mansion: condominium), T (taika: fire proof), H (hi-taika: non fire proof), 1st, 2nd and 3rd are fire classifications commonly used in Japan. According to the general descriptions of these classes, predominant construction types are reinforced concrete for M and 1st and wood for H and 3rd. Overall, both sources suggest comparable unit costs.

Table 4.1. Floor unit cost assumptions JPY Thousand

	Construction Year Book 7 Yr Average								Mitsui Sumitomo Insurance Handbook					
	Residential				Commercial				Residential			Commercial		
Prefecture	RC	ST	Wood	LM	RC	ST	Wood	LM	M	T	H	1st	2nd	3rd
Iwate	155	159	135	142	184	166	138	127	161	164	147	170	146	139
Miyagi	156	162	143	148	185	167	137	129	183	169	145	193	150	137
Tokyo	204	211	172	184	234	225	161	180	242	235	177	255	209	167
Shizuoka	175	181	159	166	223	201	173	152	197	164	168	208	146	159

For case studies that will be discussed in Section 5, a location-level high resolution exposure was generated in all coastal cities/wards by using commercially-available maps and satellite imagery. Figure 4.1 shows a snapshot of the high resolution data set, in which each point represents a building. Location-level exposure is essential for perils related to water damage such as tsunami, surge and flood that are very sensitive to location and elevation.

4.2. Inventory Development

The high resolution economic exposure based on the building footprint database has key primary building characteristics, such as occupancy type and number of stories. However, construction information is not available. In order to compute property losses, the model has to identify either a unique damage function (based on construction class) or generate a composite damage function based on available information for a given location. We created a region-specific building inventory database to support this process. The resulting composite vulnerability function represents the average vulnerability of those building types associated with the specified primary building characteristics in the region. Similar to the unit cost development, floor areas and project costs from the construction year books were used extensively to develop the inventory database, which consists of three regional inventory distributions (Urban, Sub-Urban, Rural) by occupancy. For example, Figure 4.2 shows construction class assumptions for commercial low-rise buildings in the “Urban” zone.

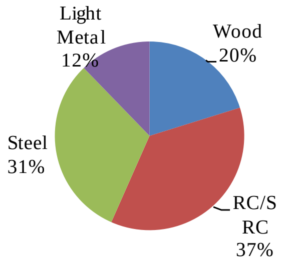

Figure 4.2. Urban area, commercial low-rise, construction assumption

4.3. Insured Exposure Assumption

For this analysis, the focus is on analyzing insured losses to the residential line of business. In Japan, residential earthquake insurance is offered as an endorsement to the fire insurance policy, which covers buildings and contents. The policy holder is required to set the amount insured under earthquake insurance within a range of 30-50%. Limits are JPY50M and 10M for building and contents, respectively. Insurance claims are paid to the policy holders based on the assigned damage states as prescribed in Earthquake Insurance Law in Japan (Total: 100%, half: 50% and partial: 5%). The damage state simply determines the percentage to multiply by the total insured amount. Accordingly, modelled mean damage ratios are translated into damage states and then associated predefined loss ratios are multiplied by 40% of total property values to compute residential insured losses. Prefecture-level earthquake insurance penetration rates published by the General Insurance Association of Japan were also applied (Aomori: 15.3%; Iwate: 13.2%; Miyagi: 33%; Fukushima: 14.6%, Shizuoka: 25%, Aichi: 35% and Osaka: 25% as of 2010).

5. CASE STUDIES

With the information on the exposure and vulnerability, we now describe the tsunami hazard footprint development, which includes inundation footprints for the Tohoku earthquake as well as realizations of tsunami-generating events on the Nankai Trough.

5.1. Methodology and Background

The inundation methodology is a modified bathtub approach based in GIS, utilizing a 100m Digital Terrain Model (DTM) for primary inundation constraints and 50m Land Cover (LULC) to add constraints on maximum wave attenuation by using the land cover as a proxy for the impact of surface roughness on a shallow wave. A cost-distance routine was employed from an ocean side starting mesh to ensure contiguous wave propagation and to avoid orphaned areas below the estimated top of wave elevation. Using historical observations of tsunami inundation extents and top of wave observations, coastal regions were assigned an estimated top of wave elevation for a given scenario. These regions defined an area of interest (AOI) from which each of the DTM, LULC and starting mesh grids were extracted. From this subset of data, a cost-distance analysis was performed across the DTM-LULC intersection within the DTM that are at or below the defined top of wave and finally limited to a cost that reflects the estimated maximum expected inundation for the given inputs. While this method does not fully capture all of the aspects of fluid dynamics and shallow water wave propagation theory, given the high level of uncertainty in historical event observations, it is a reasonable approximation when compared to extents of more recent and well-documented events (e.g., 2011 Tohoku earthquake). The inundation extents and depths defined by this method tend to be somewhat conservative by design. This is due in part to the lack of impact of coastal defences. It is assumed that the tsunami event is generated from a localized high magnitude earthquake and that many of these defences should be considered damaged or destroyed from localized shaking and ground failure, thus offering little to no protection from the incoming wave. The historical observations used for generating the top of wave estimates also add to the uncertainty of the model. Over time, the terrain across which the wave originally travelled changes – either in elevation, slope, roughness (use), distance to coast, protection, or some subset of these. The bathymetry off the coast may also have changed by subsidence, submarine landslide or earthquake activity.

5.2. Event Selection

For the tsunami scenario analyses, events were chosen to reflect the segmentation boundaries of the components of the Nankai Trough: Nankai, Tonankai and Tokai. The coastal inundation heights for the Nankai and Tonankai scenarios were informed by the events in 1944 and 1946. As there have been no recent historical events on the Tokai segment, the 1854 earthquake that ruptured both the Tonankai and Tokai was examined. Coastal inundation heights from the 1854 event were significantly higher than the 1946 Tonankai tsunami. As a result, two tsunami footprints were developed for Tokai: one with coastal inundation heights informed by the 1854 Tonankai earthquake (Tokai-high scenario) and one with inundation heights more comparable with those observed in the Nankai and Tonankai regions in 1944 and 1946 (Tokai-medium scenario). Figures 5.1 and 5.2 show the tsunami footprint study area and modelled tsunami heights for the ‘Tokai High’ scenario.

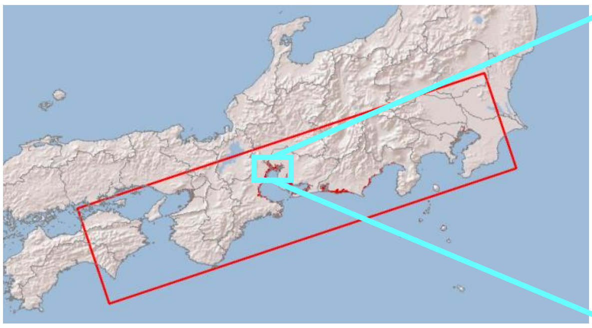

Figure 5.1. Tsunami footprint study area

Figure 5.2. Modeled tsunami height for Tokai High scenario (see Table 5.4), Nagoya vicinity

5.4. Estimated Losses for Scenario Events

A summary of losses (in JPY) using these hazard footprints with the detailed exposure and empirically-based vulnerability functions is shown in Table 5.1. These losses include building and content losses to the entire building stock (all lines), as well as the insured loss to buildings and contents for the residential line of business only. Overall, results are reasonable, though it has already been noted that there is difficulty in separating losses caused by ground shaking from those caused by tsunami. Ground shaking damage was significant in the 1944 and 1946 historical events. For the 2011 Tohoku earthquake, residential losses in Tohoku region are currently at 780 billion JPY (as of April 3, 2012). In these payouts, there is some evidence of coverage expansion, with a lack of detailed loss assessments within tsunami-inundated regions.

Table 5.1. Estimated losses for the Tohoku 2011 earthquake and historical scenarios JPY Billion

LOB	All Lines				Insured Residential Only			
Event	Bldg	Contents	Total	Exposure[1]	Bldg	Contents	Total	Exposure[1]
Tonankai Medium	1,479	1,215	2,694	18,605	696	38	734	5,486
Nankai Medium	3,106	2,434	5,540	38,333	1,363	67	1,430	11,348
Tokai Medium	2,476	1,743	4,219	12,705	1,038	63	1,101	3,847
Tokai High	8,514	5,656	14,170	52,740	3,674	168	3,842	15,848
Tohoku 2011	3,558	2,513	6,071	11,688	263	79	342	602

Notes: 1) Total exposure within footprints

6. CONCLUSIONS

This paper explores the challenges in developing vulnerability functions for tsunami hazard, as well as the detailed hydraulic modeling needed to accurately estimate hazard and detailed exposure to accurately estimate risk. To calculate tsunami risk at a location, it is necessary to understand how far the tsunami wave will propagate inland, as well as the elevations of buildings and their vulnerability to inundation. As with all flooding, risk depends on site-specific elevations and construction characteristics and high-resolution information is needed to differentiate the risk. While the vulnerability functions proposed in this paper are a good first approximation, the incorporation of a flow velocity component is needed. The authors continue to explore the development of a probabilistic tsunami model beginning with locations in the near-field of subduction zones in Japan. The 2011 Tohoku earthquake was an extreme event. However, its impacts can serve to alert the world to tsunami hazard and mitigation needs. In order to reduce the vulnerability of individuals and property on exposed coastlines around the world, protective measures are necessary.

AKCNOWLEDGEMENT

The authors sincerely thank City Bureau, MLIT and local building officials and researchers who conducted post-event field surveys in difficult conditions for directly and indirectly providing the detailed information.
Also, we would like to thank our colleagues Dr. Mohsen Rahnama and Dr. Patricia Grossi for valuable feedback and comments.

REFERENCES

N. Shuto. (1993), Tsunami intensity and disasters, Tsunamis in the World, Kluwer Academic Publishers, pp. 197-216.

H. Matsutomi, T. Sakakiyama, S. Nugroho, and M. Matsuyama. (2010). Inundation Flow Velocity of Tsunami on Land, Island Arc, Vol. 19, Issue 3, pp. 443-453.

H. Izuka and H. Matsutomi. (2000). Damage Due to Inundation Flow of Tsunami, *Proceedings of Coastal Engineering*, JSCE, 47, pp. 381-385. (in Japanese)

City Bureau, Ministy of Land, Infrastructure, Transport and Tourism. (2011) The Great East Japan Damage Survey Report Phase 2, Tokyo, Japan.

Okada. T. and Y. Nakano (1988). Reliability analysis on seismic capacity of existing reinforced concrete buildings in Japan, Proc. of 9th WCEE, VII-333-338

Beck J., Porter K., Shaikhutdinov R., Mizukoshi K., Miyamura. M., Ishida H. Moroi. T, Tukada Y. and Masuda M. (2002) Impact of seismic risk on lifetime property values, CUREE-KAJIMA JOINT RESEARCH PROGRAM, PHASE IV, pp 6-17 to 6-49, REPORT NO. EERL 2002-04

T. Hattori (1964) A Study of the damage to Houses doe to a Tsunami, Bull. Earthq. Res. Inst., Univ. Tokyo, Vul.42, pp 181-191.